Hindawi
Journal of Nanomaterials
Volume 2023, Article ID 9208703, 13 pages
https://doi.org/10.1155/2023/9208703

Research Article

Coupled Dufour and Soret Effects on Hybrid Nanofluid Flow through Gyrating Channel Subject to Chemically Reactive Arrhenius Activation Energy

Zehba Raizah,[1] **Arshad Khan**,[2] **Taza Gul**,[3] **Anwar Saeed**,[4] **Ebenezer Bonyah**,[5] **and Ahmed M. Galal**[6,7]

[1]*Department of Mathematics, College of Science, King Khalid University, Abha, Saudi Arabia*
[2]*College of Aeronautical Engineering, National University of Sciences and Technology (NUST), Sector H-12, Islamabad 44000, Pakistan*
[3]*Cambridge Graphene Centre, Electrical Engineering Division, Cambridge University Engineering Department, 9 JJ Thomson Avenue, Cambridge CB3 0FA, UK*
[4]*Center of Excellence in Theoretical and Computational Science (TaCS-CoE), Faculty of Science, King Mongkut's University of Technology Thonburi (KMUTT), 126 Pracha Uthit Road, Bang Mod, Thung Khru, Bangkok 10140, Thailand*
[5]*Department of Mathematics Education, Akenten Appiah Menka University of Skills Training and Entrepreneurial Development, Kumasi, Ghana*
[6]*Department of Mechanical Engineering, College of Engineering, Prince Sattam Bin Abdulaziz University, Wadi Alddawasir 11991, Saudi Arabia*
[7]*Production Engineering and Mechanical Design Department, Faculty of Engineering, Mansoura University, P.O. Box 35516, Mansoura, Egypt*

Correspondence should be addressed to Ebenezer Bonyah; ebbonya@gmail.com

Received 20 August 2022; Accepted 29 September 2022; Published 24 April 2023

Academic Editor: Zafar Said

This study explores the magnetohydrodynamic fluid flow through two rotating plates subjected to the impact of microorganisms. The nanoparticles of copper and alumina are mixed with water for formulating hybrid nanofluid with new combination $(Cu + Al_2O_3 + H_2O)$. This new combination augments the thermal conductivity of pure fluid. The flow is influenced by the coupled effects of Dufour and Soret diffusions. The joined effects of chemically reactive activation energy have been incorporated in the mass transportation equation. A constant magnetic field has been employed to the flow field with strength B_0 in normal direction to the plates. The equations that controlled fluid flow have been transferred to dimension-free form by implementing suitable set of variables. The influence of the different factors has been examined theoretically by employing the graphical view of different flow profiles. It has been concluded in this work that, linear velocity has declined by augmentation in magnetic factor and rotational parameter whereas these factors have enhanced microrotational profiles of fluid. Higher values of radiation parameter, Dufour number, and volumetric fractions have augmented fluid's thermal profiles. The concentration of fluid has been retarded with upsurge in Soret number and chemical reaction parameter whereas growth in activation energy parameter has supported the upsurge in concentration. The rate of motile microorganisms has retarded by upsurge in the values of Lewis and Peclet numbers. It has been noticed that when K_r, M, and Re varies from 0.2 to 0.6 then in case of nanofluid, skin friction changes from 0.288 to 0.633 at $\phi_1 = 0.01$ and from 0.292 to 0.646 at $\phi_1 = 0.02$ and in case of hybrid nanofluid the variations in skin friction are from 0.328 to 0.646 at $\phi_1, \phi_2 = 0.01$ and from 0.335 to 0.703 at $\phi_1, \phi_2 = 0.02$.

1. Introduction

In the earlier times, the transfer of mass and heat has appealed the interest of research community with more significance for its important applications at industrial level. Some of these applications are electronic devices in the field of engineering, compact thermal exchangers, nuclear reactors, etc. In the combined mass and heat transfer progressions, the fluid flow is occurred due to variations in density resulted from gradient in concentration, temperature, and composition of material. The transmission of mass is caused by variation in the thermal behavior of fluid particles which is termed as Soret effect. The energy's flux occurred due to variations in concentration and termed as Dufour effect. It is worth mentioning that these effects are of more importance for transmission of mass and heat in different engineering processes. Both Dufour and Soret effects become more significant whenever some species are acquainted at the surface of fluid with density smaller than that of surrounding fluid. Numerous applications of Soret and Dufour effects can be seen in the field of combustion flames, safety reactor, solar collectors, and building energy conservations. Chamkha and Ben-Nakhi [1] investigated MHD fluid flow upon a porous semi-infinite isothermal sheet with Soret and Dufour effects. Rasool et al. [2] revealed the impact of Soret and Dufour effect upon nanofluid flow with Darcy–Forchheimer terms in the mathematical model. It has concluded that the flow of nanoparticles has declined with higher values of porosity parameter. Khan et al. [3] have introduced the Soret and Dufour effects with significant characteristics to viscous MHD fluid flow through a rotary cone by discussing its generation of entropy as well. Vafai et al. [4] have inspected about the MHD and Dufour, Sorret effects for fluid flow upon a stretching surface and have established that thermal flow rate has declined with upsurge in radiation and viscous dissipation effects. Khan et al. [5] have concluded about the flow of viscous fluid with combined influence of Soret and Dufour. The authors in this study have focused mainly upon the flow of heat mechanism and established that magnetic effects have upsurge the thermal flow rate. The thermal fluid flow for Casson fluid with ethylene glycol as pure fluid has inspected with impacts of Soret and Dufour effects by Hafeez et al. [6]. Layek et al. [7] deliberated the collective influence of Soret and Dufour on time-dependent mass and heat transfer over permeable surface. Kotnurkar and Katagi [8] have discussed the characteristics of nanofluid flow with Soret and Dufour effects.

The combination of small-sized particles in a base fluid for enhancement of its thermal flow characteristics is termed as nanofluid. The nanoparticles flow analysis has been the topic of widespread research for various investigators, as it has upgraded the thermal characteristics of thermal flow phenomena. The nanoparticles are composed of various metal oxides such as (CuO, Al_2O_3), metals such as (Cu, Au, Ag), semiconductors such as (TiO_2, SiC), nitride ceramics such as (AlN, SiN), and carbide ceramics such as (SiC, TiC). The idea of suspending nanoparticles into a base fluid was first drifted by Choi and Eastman [9]. This work has provided a new base in the field of fluid mechanics. For its significant applications in the field of engineering and at industrial level various studies have been carried out with main focus upon thermal diffusivity among the nanoparticles. Sheikholeslami et al. [10] inspected the nanofluid flow with thermal transmission through a gyrating channel by implementing the magnetic effects. It has concluded in this inspection that there has been a direct relationship between nanoparticles volume fraction and Nusselt number for both injection and suction cases. Said et al. [11] have analyzed experimentally the novel ionic nanofluid's energy storage characteristics. Sharma et al. [12] have explored contemporary advancements in the machine learning for nanofluid-based thermal transmission in the system of renewable energy. Ahmad and Khan [13] have simulated numerically the MHD Sisko nanofluid flow past a curved movable surface.

With the passage of time researchers have realized that the dispersion of two dissimilar kinds of nanoparticles in a pure fluid, results in a fluid that has higher thermal diffusion. This new class of fluid is termed as hybrid nanofluid. Islam et al. [14] deliberated the effects of Hall current for radiated hybrid nanofluid flow through a channel and have concluded that hybrid nanofluid has superior thermal flow characteristics than traditional fluid. Said et al. [15] have explored the thermal capacity for hybrid nanofluid flow for solar energy applications. Li et al. [16] deliberated the creation of entropy for hybrid nanofluid between two plates by considering the effects of Marangoni convection in the flow model with other flow conditions. It has been concluded in this work that, rate of flow transmission is at peak for greater values of exponential and thermal source sink. Said et al. [17] have used hybrid nanofluid to discuss the applications of innovative frameworks based upon the collective enhanced regressions for modeling of heat performance small-scale Rankin cycles.

In a rotating system, the flow of fluid is a natural phenomenon. Actually, these effects of rotation occur internally among a fluid's particles that augment when the fluid gets into motion. Hence in the fluid motion the natural rotation exists up to a specific range. The concept of rotating system in viscous fluid flow was floated by Taylor [18]. The investigation of rotational motion for different flow system has been conducted in detail by Greenspan [19]. The idea of rotational motion has also extended to moving disks [20]. Forbes [21] has investigated the axisymmetric flow of fluid between two plates with lower plate as static and the upper plate as rotational. Dogonchi et al. [22] inspected the influence of stretching surface upon nanofluid flow and heat conduction in rotary channel. Muhammad et al. [23] have inspected the squeezing fluid flow between rotational plates. In this work, the effects of MHD have also taken into account for flow system. Salahuddin et al. [24] have picked second-grade fluid motion through rotary plates by considering variable fluid characteristics. It has been proved in this study that diffusivity and concentration of fluid particles are related directly with thermal conductivity and thermal transmission.

The least energy required by molecules for commencement of a chemical reaction is termed as activation energy introduced by Arrhenius. Activation energy has many applications in processing of food, and emulsions of different suspensions. First result in the paper format with combine impact of activation energy was established by Bestman [25]. Khan et al. [26] have inspected the influence of Arrhenius activation energy upon MHD second-grade fluid flow in a permeable surface. The term has been also used by Bhatti and Michaelides [27] by considering its impact upon thermos-bioconvective nanofluid flow over a Riga plate and has concluded that flow profiles have been weakened by expanding values of Rayleigh number. Khan et al. [28] have deliberated a wonderful work upon hybrid nanofluid flow by considering the influence of Arrhenius activation energy upon flow system. The authors have concluded in their investigation that mass diffusivity has jumped up for expansion in activation energy parameter. More established work can be studied in previous studies [29–33].

The effects of magnetic field have a considerable part in fluid mechanics. It has numerous engineering and industrial applications for instance MHD generators and pumps, etc. Various investigations have been conducted with main emphasis upon transportation of heat with MHD effects. Shehzad et al. [34] have inspected the influence of MHD upon three-dimensional flow of Jeffery fluid with Newtonian heating effects and have revealed that fluid's motion has opposed while the thermal flow rate and skin friction have supported with augmentation in magnetic parameter. Ahmad et al. [35] have investigated unsteady MHD nanofluid flow over a cylindrical disk placed vertically. Usman et al. [36] have investigated the EMHD impact upon couple stress film flow of nanofluid over spinning disk and have calculated the percentage augmentation in thermal flow rate for single and double nanoparticles fluid flow. Ahmad and Khan [37] have inspected the significance of activation energy in the advancement of covalent bonding using Sisko MHD nanofluid flow past a moveable curved sheet. Ahmad et al. [38] have investigated thermally radiated Sisko fluid flow subject to Joule heating and MHD effects and have concluded that thermal flow has augmented with corresponding growth in radiation and magnetic factors.

From the aforementioned investigations, it has been discovered that no study has yet been steered to deliberate the thermal flow rate for hybrid nanofluid flow through rotating plates by employing the combined Dufour, Soret effects and the impact of microorganisms. The following points support the novelty of the work:

(i) Coupled Dufour and Soret effects are taken in mathematical model of flow problem.

(ii) Chemically reactive Arrhenius activation energy is also incorporated in concentration equation.

(iii) The plates at the boundaries are considered as rotating, where the spinning effects of plates are coupled in the flow equations.

(iv) The effects of microorganism has used in the modeled equations.

(v) Magnetic effect is applied to the flow system and is incorporated mathematically in momentum equations.

(vi) HAM is worked out for solution of model problem.

2. Problem Formulation

Take an incompressible viscous hybrid nanofluid fluid flow between two plates. The system of coordinates is selected so that plates along fluid are rotating with angular velocity Ω about y-axis. h is the distance between the plates such that Cu, Al_2O_3—nanoparticles are mixed with water for formulating hybrid nanofluid with combination$(Cu + Al_2O_3 + H_2O)$. The flow is influenced by the coupled effects of Dufour and Soret diffusions. The collective impact of chemically reactive Arrhenius activation energy has been incorporated in mathematical model of problem. Magnetic field has also been employed to the flow system with strength B_0 in normal direction to the plates, as shown in Figure 1. It is supposed that the existence of nanoparticles will not affect the microorganisms' direction, swimming, and their velocity.

With the help of above assumptions, one has following set of equations [14, 39, 40]:

$$\frac{\partial u}{\partial x} + \frac{\partial w}{\partial z} + \frac{\partial v}{\partial y} = 0, \tag{1}$$

$$v\frac{\partial u}{\partial y} + u\frac{\partial u}{\partial x} + 2\omega w + \frac{1}{\rho_{\mathrm{hnf}}}\frac{\partial p}{\partial x} = \frac{\mu_{\mathrm{hnf}}}{\rho_{\mathrm{hnf}}}\left(\frac{\partial^2 u}{\partial x^2} + \frac{\partial^2 u}{\partial y^2}\right) - \frac{\sigma {B_0}^2}{\rho_{\mathrm{hnf}}}u, \tag{2}$$

$$v\frac{\partial v}{\partial y} + u\frac{\partial v}{\partial x} + \frac{1}{\rho}\frac{\partial p}{\partial y} = +\frac{\mu_{\mathrm{hnf}}}{\rho_{\mathrm{hnf}}}\left(\frac{\partial^2 v}{\partial y^2} + \frac{\partial^2 v}{\partial x^2}\right), \tag{3}$$

$$u\frac{\partial w}{\partial x} + v\frac{\partial w}{\partial y} - 2\omega u = \frac{\mu_{\mathrm{hnf}}}{\rho_{\mathrm{hnf}}}\left(\frac{\partial^2 w}{\partial x^2} + \frac{\partial^2 w}{\partial y^2}\right) - \frac{\sigma {B_0}^2}{\rho_{\mathrm{hnf}}}w, \tag{4}$$

$$u\frac{\partial T}{\partial x} + v\frac{\partial T}{\partial y} + w\frac{\partial T}{\partial z} = \alpha^*\left(\frac{\partial^2 T}{\partial x^2} + \frac{\partial^2 T}{\partial y^2} + \frac{\partial^2 T}{\partial z^2}\right) - \frac{1}{\left(\rho c_{\mathrm{p}}\right)_{\mathrm{hnf}}}\frac{\partial q_r}{\partial y} + \frac{D_{\mathrm{M}}k_{\mathrm{T}}}{c_{\mathrm{s}}c_{\mathrm{p}}}\left(\frac{\partial^2 C}{\partial x^2} + \frac{\partial^2 C}{\partial y^2} + \frac{\partial^2 C}{\partial z^2}\right), \tag{5}$$

$$u\frac{\partial C}{\partial x} + v\frac{\partial C}{\partial y} + z\frac{\partial C}{\partial z} = D\left(\frac{\partial^2 C}{\partial x^2} + \frac{\partial^2 C}{\partial y^2} + \frac{\partial^2 C}{\partial z^2}\right) + \frac{D_{\mathrm{M}}k_{\mathrm{T}}}{T_{\mathrm{m}}}\left(\frac{\partial^2 T}{\partial x^2} + \frac{\partial^2 T}{\partial y^2} + \frac{\partial^2 T}{\partial z^2}\right) - {k_{\mathrm{r}}}^2(C - C_h)\left(\frac{T}{T_h}\right)^n \exp\left(-\frac{E_a}{k_{\mathrm{B}}T}\right), \tag{6}$$

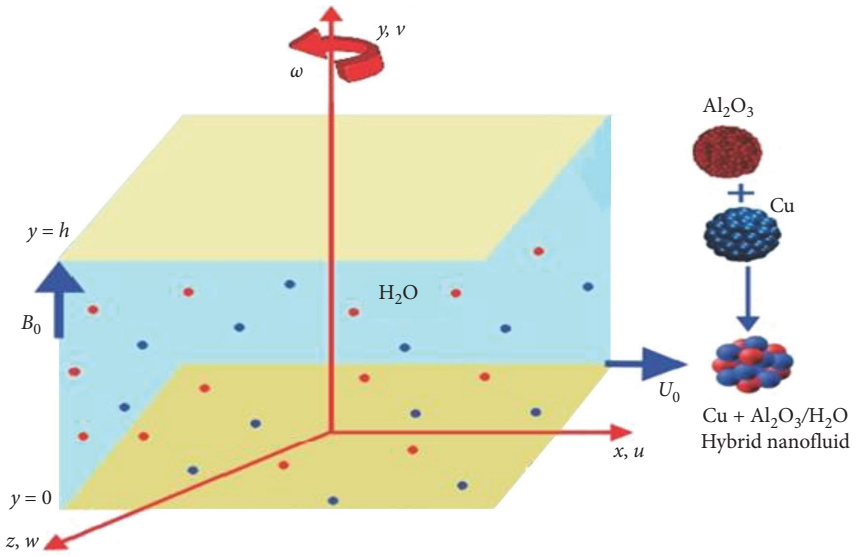

FIGURE 1: Physical view of flow problem.

$$u\frac{\partial n}{\partial x}+v\frac{\partial n}{\partial y}+w\frac{\partial n}{\partial z}+\left(\frac{bW_c}{C_b-C_t}\right)\frac{\partial}{\partial y}\left(n\frac{\partial C}{\partial y}\right)=D_m\left(\frac{\partial^2 n}{\partial x^2}+\frac{\partial^2 n}{\partial y^2}+\frac{\partial^2 n}{\partial z^2}\right). \tag{7}$$

Above, the flow components u, v, w are, respectively, along coordinate axes; μ_{hnf}, ρ_{hnf} are the dynamic viscosity and density of hybrid nanofluid, ω is the angular velocity, q_r is the heat flux due to radiation, $(\rho c_p)_{hnf}$ is heat capacitance, $\alpha^* = k_{hnf}/(\rho C_p)_{hnf}$ is the thermal diffusion in which k_{hnf} is thermal conductance of nanofluid, D_M is mass diffusivity, k_T is ratio of thermal diffusion, D_m is diffusion of microorganism, C_0 and T_0 are the concentration and temperature at lower plate of channel while C_h and T_h are the corresponding quantities at the upper plate. Moreover, $(T/T_t)^n e^{(-E_a/k_B T)}$ is modified Arrhenius function, W_c is speed of microorganism cells, E_a is activation energy, and $k_r{}^2$ is the rate of reaction.

Conditions at boundaries are:

$$\begin{aligned} &u = ax,\ w = 0,\ v = 0,\ C = C_0,\ T = T_0,\ n = n_0,\ \text{at } y = 0\\ &u = 0,\ w = 0,\ v = 0,\ C = C_h,\ T = T_h,\ n = n_h,\ \text{at } y = h. \end{aligned} \tag{8}$$

Use the following set of suitable transformations [41, 42]:

$$\begin{aligned} &u = axf'(\eta);\quad v = -ahf(\eta);\quad w = axg(\eta);\quad \chi(\eta) = \frac{n-n_h}{n_0-n_h};\\ &\theta(\eta) = \frac{T-T_h}{T_0-T_h};\quad \phi(\eta) = \frac{C-C_h}{C_0-C_h};\quad \text{with } \eta = \frac{y}{h}. \end{aligned} \tag{9}$$

For simplification of q_r use the Rosseland approximation as given in Equation (10) [43, 44]:

$$q_r = -\frac{4}{3}\left(\frac{\sigma^* \partial T^4}{\kappa^* \partial \hat{y}}\right). \tag{10}$$

In Equation (10), σ^*, κ^* are termed as Stefan Boltzmann constant and coefficient of Rosseland mean absorption such that $\sigma^* = 5.6697 \times 10^{-8}\ \text{Wm}^{-2}\ \text{K}^{-4}$. If the thermal gradient is sufficiently small within the flow of fluid then T^4 can be simplified by using Taylor's expansion as [44]:

$$T^4 \cong 4TT_h{}^3 - T_h{}^4. \tag{11}$$

In light of Equations (10) and (11), we have from Equation (5) as:

$$\begin{aligned} u\frac{\partial T}{\partial x}+v\frac{\partial T}{\partial y}+w\frac{\partial T}{\partial z} = {}& \alpha^*\left(\frac{\partial^2 T}{\partial x^2}+\frac{\partial^2 T}{\partial y^2}+\frac{\partial^2 T}{\partial z^2}\right)\\ &+\frac{1}{(\rho c_p)_{hnf}}\left(\frac{16\sigma^*}{3k^*}T_h{}^3\frac{\partial^2 T}{\partial y^z}\right)\\ &+\frac{Dk_T}{c_s c_p}\left(\frac{\partial^2 C}{\partial x^2}+\frac{\partial^2 C}{\partial y^2}+\frac{\partial^2 C}{\partial z^2}\right). \end{aligned} \tag{12}$$

In light of Equation (9), we have from Equations (1–4, 6, 7 and 12) in dimensionless form as follows:

$$\begin{aligned} &\{(1-\phi_1)(1-\phi_2)\}^{-2.5} f^{(iv)}\\ &+\left\{(1-\phi_2)\left((1-\phi_1)+\phi_1\frac{\rho_{s1}}{\rho_f}\right)+\phi_2\frac{\rho_{s2}}{\rho_f}\right\}\\ &(\text{Re}(ff''' - f'f'')) - 2K_r g' - Mf'' = 0 \end{aligned} \tag{13}$$

Table 1: Numerical values of base fluid and nanoparticles for thermophysical characteristics.

Properties	Cu-nanoparticles	Al_2O_3-nanoparticles	H_2O-base fluid
$\rho\ (\mathrm{kg\cdot m^{-3}})$	8,933.00	3,970.00	997.10
$C_p\ (\mathrm{J\cdot kg^{-1}\cdot K^{-1}})$	385.00	765.00	4,179.00
$\kappa\ (\mathrm{W\cdot m^{-1}K^{-1}})$	400.00	40.00	0.613.00

$$\begin{aligned}&\{(1-\phi_1)(1-\phi_2)\}^{-2.5}g''\\&-\left\{(1-\phi_2)\left((1-\phi_1)+\phi_1\frac{\rho_{s1}}{\rho_f}\right)+\phi_2\frac{\rho_{s2}}{\rho_f}\right\}\\&(\mathrm{Re}(f'g-fg')-2K_{\mathrm{r}}f')-\mathrm{Mg}=0\end{aligned}\tag{14}$$

$$\begin{aligned}&\frac{k_{nf}}{k_f}\left(1+\frac{4}{3}\mathrm{Rd}\right)\theta''+\left\{(1-\phi_2)\left((1-\phi_1)+\phi_1\frac{\rho_{s1}}{\rho_f}\right)+\phi_2\frac{\rho_{s2}}{\rho_f}\right\}\\&\mathrm{Pr}(\mathrm{Re}\,\theta'f'+\mathrm{Du}\,\phi'')=0\end{aligned}\tag{15}$$

$$\phi''-\mathrm{Sc}\phi'+\mathrm{ScSr}\,\theta''-\mathrm{Sc}\,\Gamma(1+\tau\theta)^n\ \exp\left(\frac{-E}{1+\tau\theta}\right)\phi=0\tag{16}$$

$$\chi''-\mathrm{Re}Lbf\chi'+\mathrm{Pe}[\chi'\phi'+(\delta+\chi)\phi'']=0.\tag{17}$$

Above, Re is Reynolds number, K_{r} is rotation parameter, M is magnetic parameter, Pr is Prandtl number, Rd is radiation parameter, Du is Dufour number, E is activation energy parameter, τ is temperature parameter, Sr is Soret number, Γ is chemical reaction parameter, Sc is Schmidt number Lb,Pe are bioconvection Lewis and Peclet numbers. These parameters are mathematically described as:

$$\begin{aligned}&\mathrm{Re}=\frac{ah^2}{\upsilon_f},\ \ K_{\mathrm{r}}=\frac{\omega h^2}{\upsilon_f},\ \ M=\frac{h^2\sigma_f{B_0}^2}{\mu_f},\ \mathrm{Pr}=\frac{\mu_f(C_p)_f}{k_f},\\&\mathrm{Rd}=4\frac{\sigma^*}{k^*k_{\mathrm{hnf}}}{T_h}^3,\ \ \Gamma=\frac{{K_{\mathrm{r}}}^2h^2}{\upsilon_f},\ \ \mathrm{Lb}=\frac{\upsilon_f}{D_{\mathrm{M}}},\\&\mathrm{Du}=\frac{D_{\mathrm{M}}k_{\mathrm{T}}}{C_sC_{\mathrm{p}}}\frac{(C_0-C_h)}{(T_0-T_h)},\ \ E=\frac{E_a}{k_BT_h},\ \ \tau=\frac{T_0-T_h}{T_h},\\&\mathrm{Sr}=\frac{D_{\mathrm{M}}k_{\mathrm{T}}}{T_{\mathrm{M}}\upsilon_f}\frac{(T_0-T_h)}{(C_0-C_h)},\ \ \mathrm{Sc}=\frac{\upsilon_f}{D_{\mathrm{M}}},\ \ \mathrm{Pe}=\frac{bW_{\mathrm{c}}}{D_{\mathrm{M}}}.\end{aligned}\tag{18}$$

The thermos-physical characteristics of solid nanoparticles are defined as follows with its numerical values are depicted in Table 1:

$$\begin{aligned}\mu_{\mathrm{hnf}}&=\frac{\mu_f}{\{(1-\phi_1)(1-\phi_2)\}^{2.5}},\\\rho_{\mathrm{hnf}}&=\left\{(1-\phi_2)\left((1-\phi_1)+\phi_1\frac{\rho_{s1}}{\rho_f}\right)+\phi_2\frac{\rho_{s2}}{\rho_f}\right\}\rho_f,\\(\rho C_{\mathrm{p}})_{\mathrm{hnf}}&=\left\{(1-\phi_2)\left((1-\phi_1)+\phi_1\frac{(\rho C_{\mathrm{p}})_{s1}}{(\rho C_{\mathrm{p}})_f}\right)\right.\\&\quad\left.+\phi_2\frac{(\rho C_{\mathrm{p}})_{s2}}{(\rho C_{\mathrm{p}})_f}\right\}(\rho C_{\mathrm{p}})_f,\\\kappa_{\mathrm{hnf}}&=\frac{\kappa_{s2}+2\kappa_f-2\phi_2(\kappa_f-\kappa_{s2})}{\kappa_{s2}+2\kappa_f+\phi_2(\kappa_f-\kappa_{s2})}\kappa_{\mathrm{nf}}.\end{aligned}\tag{19}$$

The related conditions at the boundaries are:

$$\begin{aligned}&f(0)=0,g(0)=0,f'(0)=1,\theta(0)=1,\phi(0)=1,n(0)=1\ \text{at}\ \eta=0,\\&f(1)=0,g(1)=0,f'(1)=0,\theta(1)=0,\phi(1)=0,n(1)=0\ \text{at}\ \eta=h.\end{aligned}\tag{20}$$

2.1. Physical Quantities. In the problems related to thermodynamics, the engineers and scientists are normally interested to determine the thermal and mass flow rates for fluid flow system. In this regard, some quantities of interest are depicted in Equation (21):

$$\begin{aligned}C_f&=\frac{h\mu_{\mathrm{nf}}}{\rho_fu}.\frac{\partial u}{\partial y}\Big|_{\,y=0},\\\mathrm{Nu}&=\frac{h}{k_f(T_0-T_h)}\left(k_{\mathrm{hnf}}+\frac{16\sigma^*{T_h}^3}{3k^*}\right)\frac{\partial T}{\partial y}\Big|_{\,y=0},\\\mathrm{Sh}&=-\frac{h}{(C_0-C_h)}\frac{\partial C}{\partial y}\Big|_{\,y=0},\\\mathrm{Nn}&=\frac{x}{D_m(n_{\mathrm{b}}-n_{\mathrm{t}})}\left\{-D_{\mathrm{m}}\frac{\partial n}{\partial y}\Big|_{\,y=0}\right\}.\end{aligned}\tag{21}$$

Incorporating Equation (9) in Equation (21), the resultant equation in refined form is expressed as:

$$\begin{aligned}&C_{\mathrm{f}}=(1-\phi_1-\phi_2)^{2.5}f''(0),\ \ \mathrm{Nu}=\frac{k_{\mathrm{hnf}}}{k_f}\left(1+\frac{4}{3}\mathrm{Rd}\right)\theta'(0),\\&\mathrm{Sh}=-\phi'(0),\ \ \mathrm{Nn}=-\chi'(0).\end{aligned}\tag{22}$$

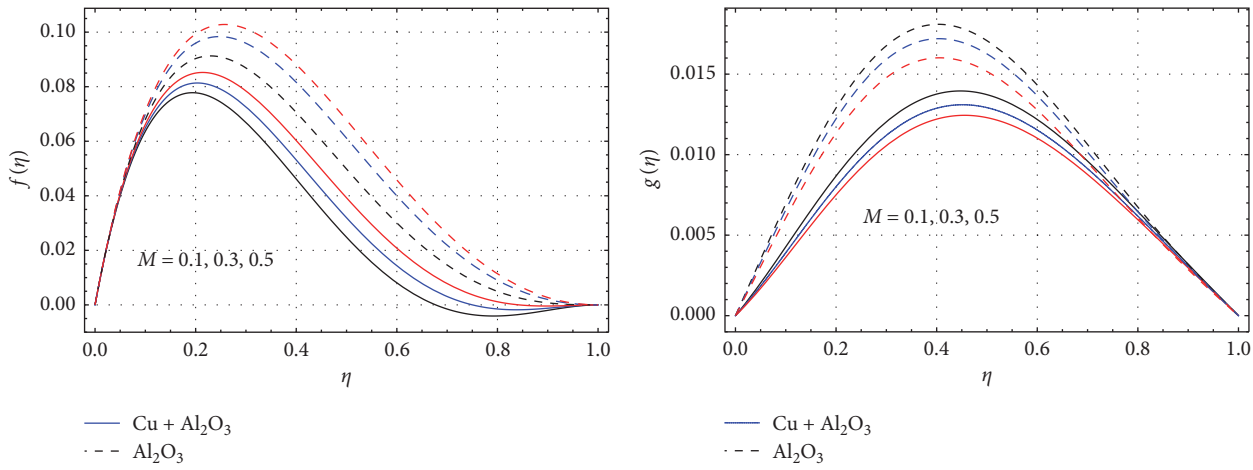

FIGURE 2: Linear and microrotation velocities vs. variations in M.

3. Problem Solution

For solution of modeled equations, the semianalytical technique HAM [45, 46] will be incorporated. This technique describes the solution in the form of functions and is most suitable for solving nonlinear equations. To solve Equations (13–17) by considering boundary conditions in Equation (20), we shall start with the following initial guesses:

$$\widehat{f}_0(\eta) = (\gamma + 2\lambda - 2\alpha + \beta)\eta^3 + (3\alpha - \beta - 2\lambda - 2\gamma)\eta^2 + \lambda\eta - \alpha$$

$$\widehat{\Theta}_0(\eta) = 1 - \eta, \quad \widehat{\Phi}_0(\eta) = 1 - \eta, \quad \widehat{\chi}_0(\eta) = 1 - \eta, \tag{23}$$

whereas the linear operators are described as:

$$L_f(f) = f''' - f', \quad L_\Theta(\Theta) = \theta'' - \theta,$$
$$L_\Phi(\Phi) = \phi'' - \phi, \quad L_\chi(\chi) = \chi'' - \chi. \tag{24}$$

The relations in Equation (24) can be mathematically described as:

$$L_f(d_1 + d_2e^{\eta} + d_3e^{-\eta}) = 0, \quad L_\Theta(d_4e^{\eta} + d_5e^{-\eta}) = 0,$$
$$L_\Phi(d_6e^{\eta} + d_7e^{-\eta}) = 0, \quad L_\chi(d_8e^{\eta} + d_9e^{-\eta}) = 0. \tag{25}$$

In Equation (25), d_i for $i = 1, 2, 3.....9$ are constants.

4. Results and Discussion

In this work, an attempt is made to explore the characteristics of magnetohydrodynamic hybrid nanofluid flow through two rotating plates. The flow is influenced by the coupled effects of Dufour and Soret diffusions and motile microorganisms. Magnetic field has employed to the flow system with strength B_0 in normal direction to the plates. The system of equations is shifted to dimension-free format by using suitable variables. Various nondimensional factors have been encountered in the process of nondimensionalization which will be discussed in the forthcoming sections.

4.1. Effects of Emerging Parameters on $f(\eta)$ and $g(\eta)$ Profiles. In Figures 2(a) and 2(b), the effect of magnetic factor M upon $f(\eta)$ and $g(\eta)$ is portrayed. Clearly an expansion in M results the creation of Lorentz force in the fluid motion and offer more resistance to linear velocity. In this process, swirling motion is supported by Lorentz force. Hence, the higher values of M decline $f(\eta)$, as shown in Figure 2(a) and augment the profiles of $g(\eta)$, as shown in Figure 2(b). The impact is more significant for hybrid nanoparticles than traditional nanoparticles. The influence of rotational parameter K_r upon $f(\eta)$ and $g(\eta)$ is shown in Figures 3(a) and 3(b). Since augmentation in K_r supports the rotational behavior and opposing linear behavior of fluid motion, hence, higher values of K_r-retard fluid motion $f(\eta)$ and augment $g(\eta)$, as shown in Figures 3(a) and 3(b). From Figures 4(a) and 4(b), it has been noticed that augmentation in volumetric fractions ϕ_1, ϕ_2 retarded the fluid motion linearly and rotationally. This phenomenon can be explained as, with augmentation in ϕ_1, ϕ_2, the dense behavior of nanoparticles enhanced within the fluid motion due to which more constraint is experienced by fluid motion. As a result, the velocity profiles declined in all directions. Since with higher values of Re the viscous forces become dominant due to which fluid motion tends to condense. Hence, the linear as well as microrational velocity profiles retarded for growth in Re, as shown in Figures 5(a) and 5(b).

4.2. Effects of Different Emerging Parameters on Temperature Profiles $\theta(\eta)$. The influence of different emerging factors upon thermal profiles has shown in Figure 6(a)–6(c). The growing values of Dufour number Du results an augmentation in thermal flow of fluid. Actually, for higher values of Du, maximum energy transfer takes place from higher to lower concentration zone, hence, causing a growth in thermal profiles, as shown in Figure 6(a). The higher values of ϕ_1 and ϕ_2 are responsible for generation of more friction to

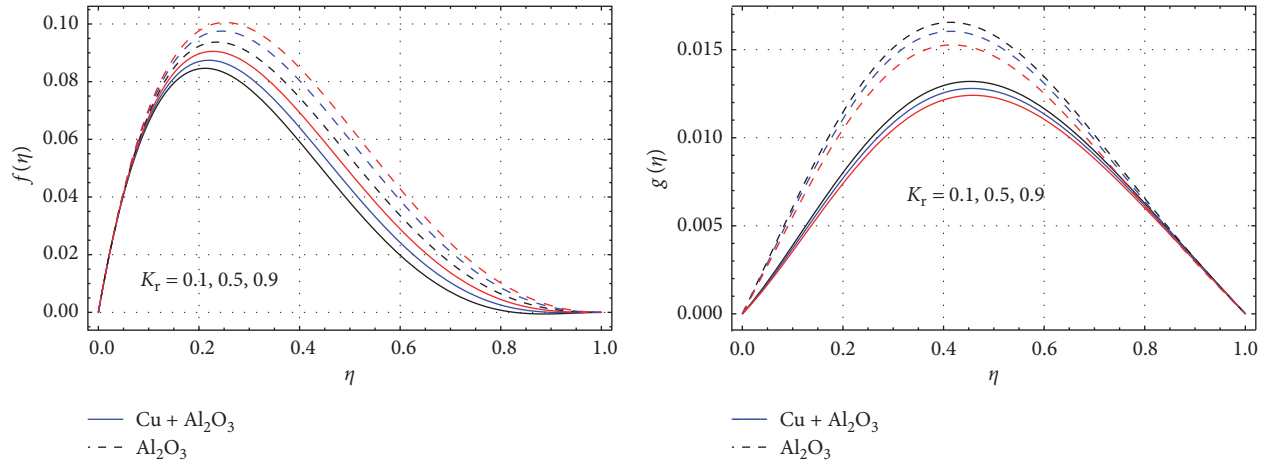

Figure 3: Linear and microrotation velocities vs. variations in K_r.

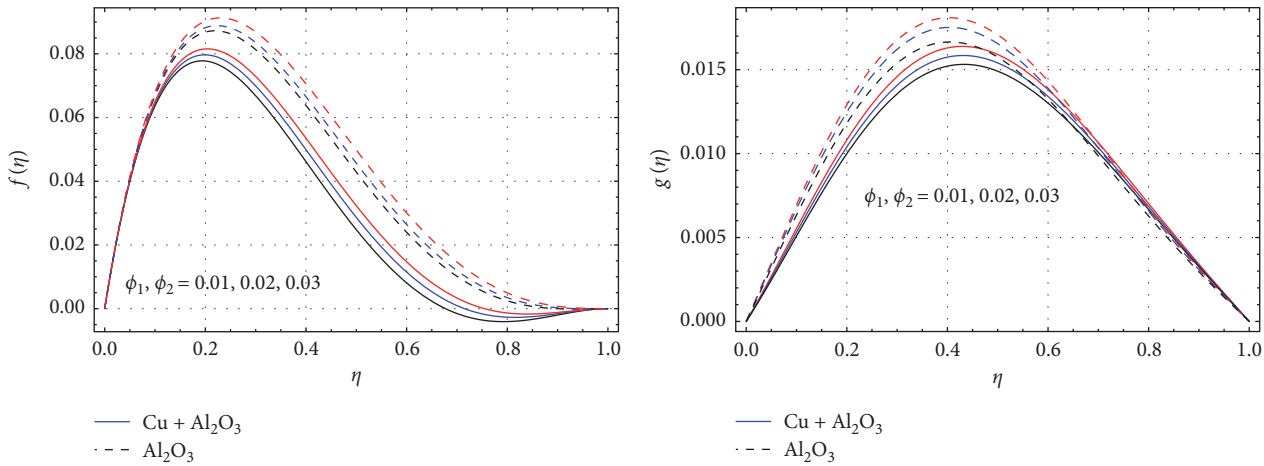

Figure 4: Linear and microrotation velocities vs. variations in ϕ_1 and ϕ_2.

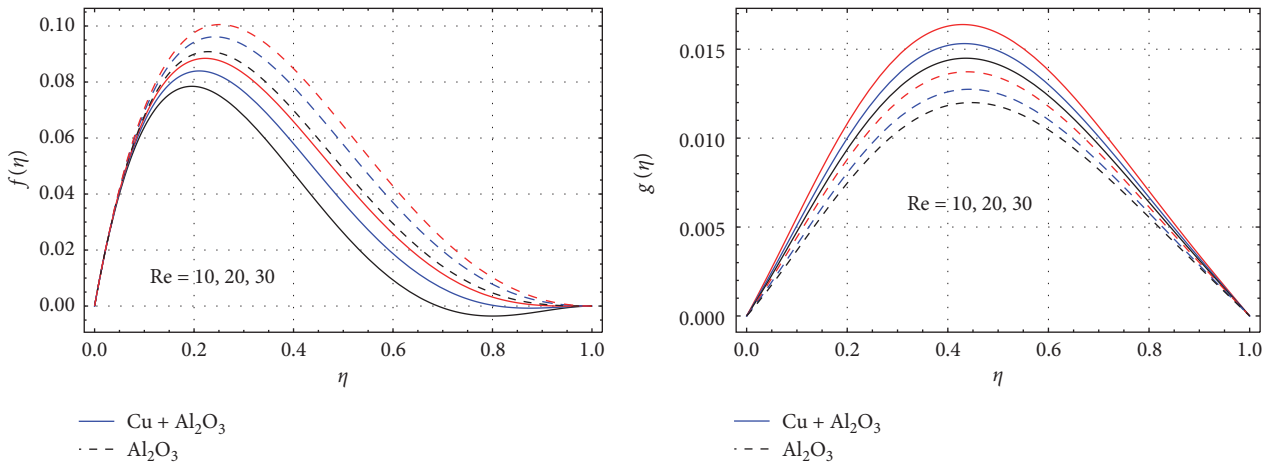

Figure 5: Linear and microrotation velocities vs. variations in Re.

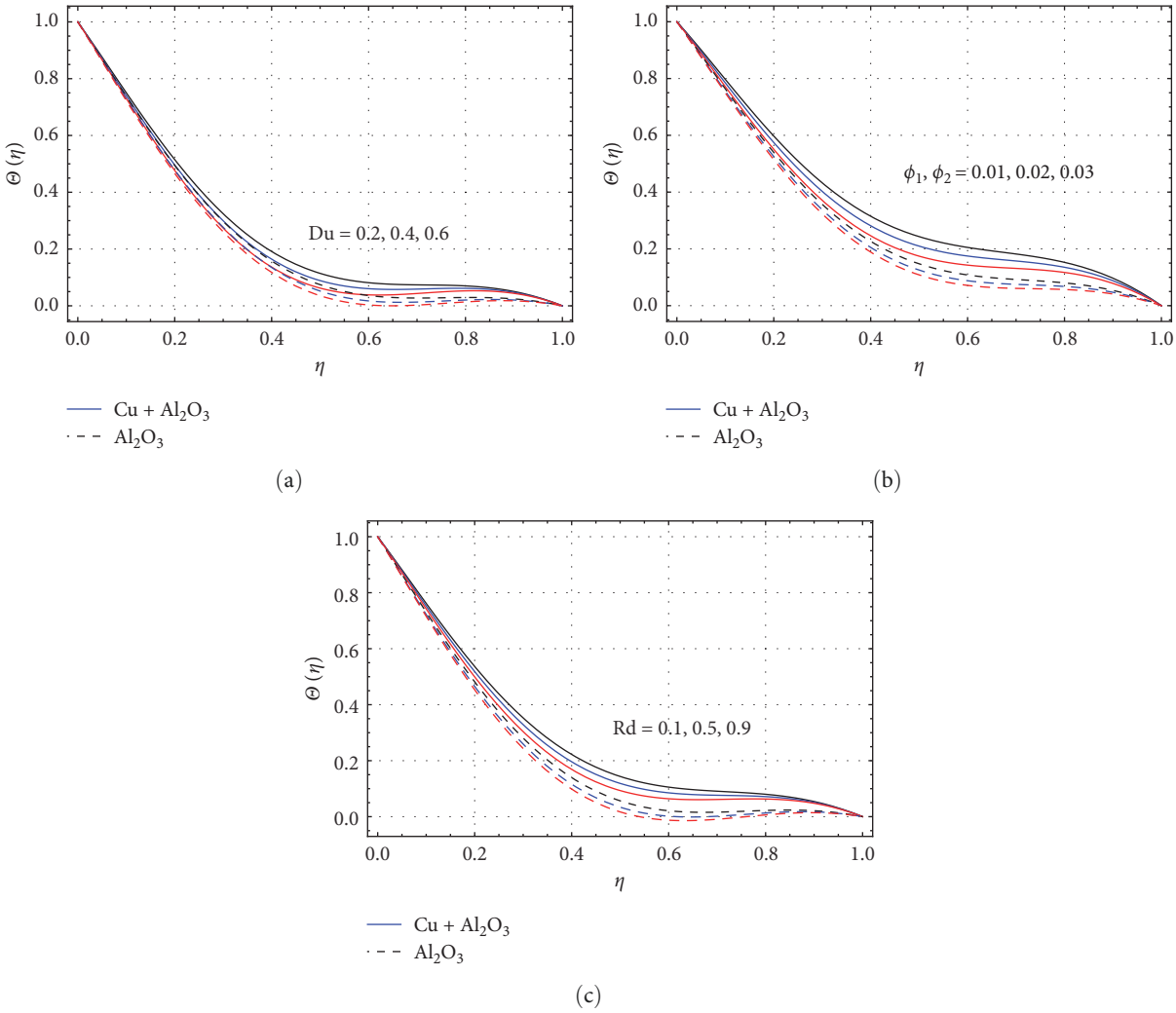

FIGURE 6: Variations in temperature vs. variations in Du, (ϕ_1, ϕ_2), and Rd.

fluid flow in response of resistance to fluid motion. In this process, kinetic energy of fluid particles converted to heat energy that overshoot the thermal flow of fluid, as shown in Figure 6(b). Figure 6(c) shows that augmentation in radiation factor Rd is responsible for growth in temperature. Actually, for higher values of Rd, the thickness of thermal boundary layer grows up due to more transportation of heat that augments the thermal profiles.

4.3. Effects of Different Emerging Parameters on Concentration Profiles $\Phi(\eta)$. The influences of various emerging parameters upon concentration profiles have been shown in Figure 7(a)–7(c). Since the Soret number is mathematically expressed as $\mathrm{Sr} = D_{\mathrm{M}} k_{\mathrm{T}}.(T_0 - T_h)/T_{\mathrm{M}} \upsilon_f.(C_0 - C_h)$, so with upsurge in the values of Sr, the concentration gradient of the fluid flow system will decline due to which less mass diffusivity will occur. In this process, the concentration of the flow system retards, as shown in Figure 7(a). It has been perceived from Figure 7(b) that higher values of activation energy factor E support the mass diffusion. Physically, it can be explained as, a growth in the values of E shoots-up the concentration of molecules with less requisite energy and causes more transportation of mass for fluid flow system that ultimately strengthens the thickness of boundary layer for concentration. In this phenomenon concentration profiles upsurge, as shown in Figure 7(b). The higher values of chemical reaction factor Γ drop the mass diffusion, as shown in Figure 7(c). Actually, with upsurge in Γ, the chemical molecular diffusion declines due to which less diffusion of mass occurs and ultimately retards the concentration profiles.

4.4. Effects of Different Emerging Parameters on Microorganism Profiles $\chi(\eta)$. The influence of bioconvection-Lewis and Peclet numbers (Lb,Pe) over microorganism profiles is shown in Figures 8(a) and 8(b). The augmenting values of both these two parameters weakens the boundary layer thickness of microorganisms due to which less mass diffusions of motile microorganism take place, as shown in Figures 8(a) and 8(b).

4.5. Table Discussions. In Table 1, the thermophysical characteristics for different nanoparticles and base fluid have been depicted numerically. In Tables 2–5, the influence of different emerging parameters has been presented numerically upon various quantities of interest. Since magnetic factor, rotational and viscous parameters are responsible for

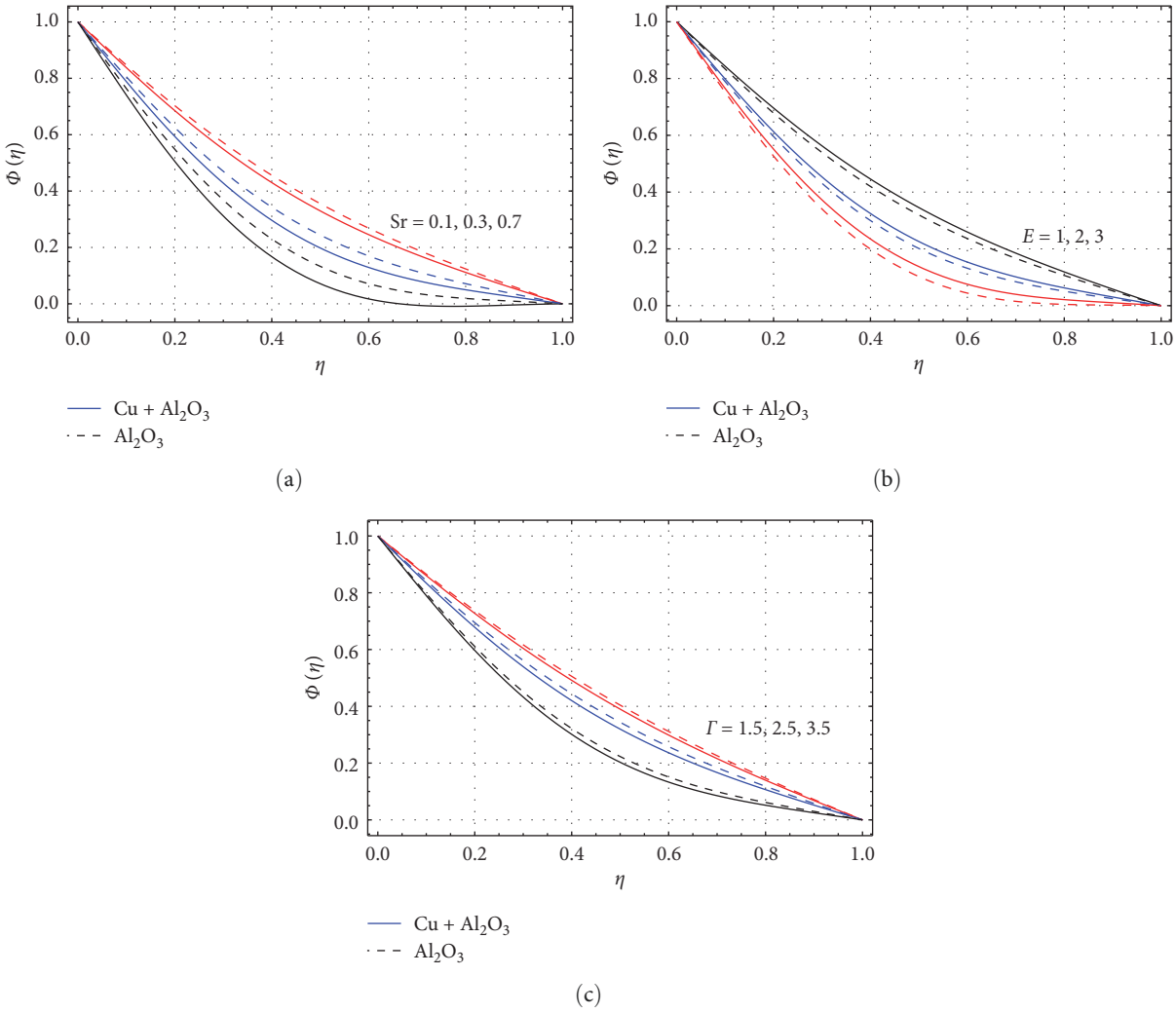

Figure 7: Variations in concentration vs. variations in Sr, E, and Γ.

resistance to fluid flow due to which maximum friction has experienced by fluid's particles. Hence, with growth in these three factors the skin friction grows up as depicted in Table 2. This impact is more visible for hybrid nanoparticles as compared to traditional or single nanoparticles. Table 3 depicts numerically the influence of magnetic, radiation factors, and Dufour number. It is obvious from this table that Nusselt number has increased with growth in radiation parameter whereas upsurge in magnetic parameter and Dufour number has an adverse effect upon Nusselt number. Again the impact is more visible in case of hybrid nanofluid. Table 4 depicts that growing values of Schmidt number upsurge the Sherwood number whereas growing values of Dufour, Soret numbers, and energy activation parameter have declined it. From Table 5 it has revealed that higher values of Lewis and Peclet numbers enhanced the motile rate.

5. Conclusion

This study explores the MHD fluid flow through two rotating plates subject to the effects of microorganisms. The copper and alumina nanoparticles have been mixed with water for formulating hybrid nanofluid. This new combination augments the thermal conductivity of pure fluid. The flow is influenced by the coupled effects of Dufour and Soret diffusions. The joined effects of chemically reactive activation energy have been incorporated in the mass transportation equation. Magnetic effects have been employed to the flow system with strength B_0 in normal direction to the plates. The impact of the embedded parameters has been examined theoretically by employing the graphical view of different flow profiles. After detailed study of the article, it has revealed that:

(i) Linear velocity has declined by augmentation in magnetic factor and rotational parameters, whereas these factors have enhanced microrotational profiles of fluid.

(ii) Augmentation in viscosity parameter and volumetric fractions has declined the fluid motion in all directions.

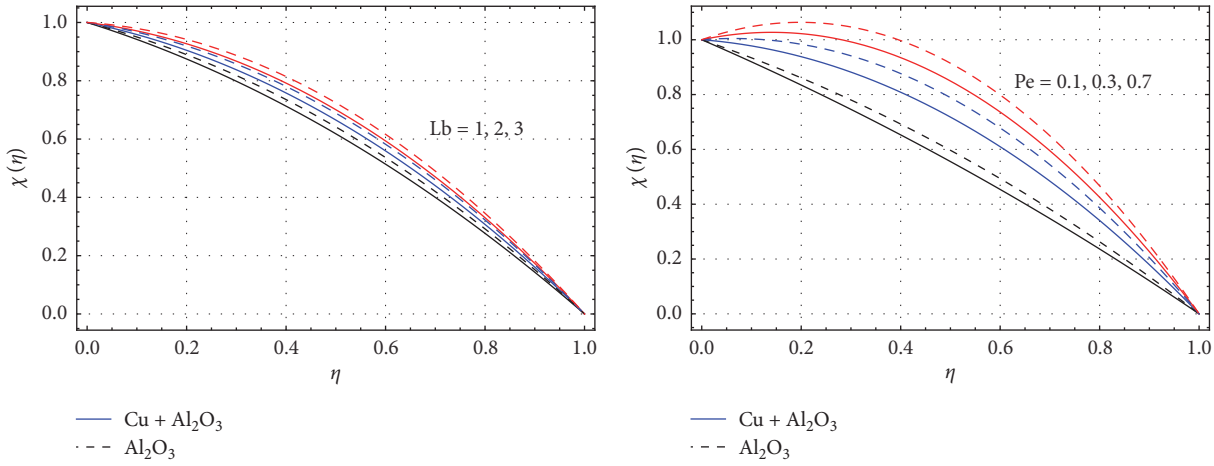

Figure 8: Variations in $\chi(\eta)$ vs. variations in Lb and Pe.

Table 2: Influence of various parameters on skin friction coefficient $-f''(0)$ at lower plate.

K_r	M	Re	$-f''(0)$ $\phi_1 = 0.01$ Nanofluid	$-f''(0)$ $\phi_1, \phi_2 = 0.01$ Hybrid nanofluid	$-f''(0)$ $\phi_1 = 0.02$ Nanofluid	$-f''(0)$ $\phi_1, \phi_2 = 0.02$ Hybrid nanofluid
0.2	0.2	0.2	0.287654	0.3276321	0.29210876	0.33522763
0.4			0.31874532	0.345218745	0.327658745	0.35410452
0.6			0.34568321	0.36543456	0.353256832	0.376426543
	0.4		0.29821087	0.31298210	0.301298210	0.320217129
	0.6		0.3082861	0.33287828	0.31728286	0.34321328
		0.4	0.42765431	0.46743276	0.435427654	0.47542674
		0.6	0.6328761	0.695423287	0.64572876	0.70251954

Table 3: Influence of nanofluid and hybrid nanofluid versus Nusselt number.

Rd	M	Du	$-\theta'(0)$ $\phi_1 = 0.01$ Nanofluid	$-\theta'(0)$ $\phi_1, \phi_2 = 0.01$ Hybrid nanofluid	$-\theta'(0)$ $\phi_1 = 0.03$ Nanofluid	$-\theta'(0)$ $\phi_1, \phi_2 = 0.03$ Hybrid nanofluid
0.2	0.2	0.4	2.46210	2.5203462	2.5421462	2.632152034
0.4			2.698210	2.7421698	2.7532698	2.852374216
0.6			2.8732102	2.94218732	2.9231873	3.103942187
	0.4		2.6732107	2.7356732	2.7724673	2.85473567
	0.6		2.68921255	2.7016892	2.8268921	2.89670168
		0.6	2.21087	2.23421087	2.3232108	2.321234210
		0.8	2.1065922	2.14108065	2.2010659	2.210141080

Table 4: Influence of nanofluid and hybrid nanofluid versus Sherwood number.

Sc	Sr	Du	E	$-\phi'(0)$ Nanofluid	$-\phi'(0)$ Hybrid nanofluid
2	1	1	1	4.63289143	4.673421
3				4.972910	5.0132097
4				5.43210	5.4929432
	2			4.762019	4.78210762
	3			4.89201	4.9432892
		2		4.983201	5.1209832
		3		5.520123	5.6321520
			2	4.103721	4.1215037
			3	3.832019	3.7323201

Table 5: Influence of nanofluid and hybrid nanofluid versus motile rate.

Lb	Pe	$-\chi'(0)$ Nanofluid	$-\chi'(0)$ Hybrid nanofluid
2	2	5.32172744	5.34322172
3		5.3673215	5.38673215
4		5.4227663	5.445227663
	3	5.465321325	5.474653213
	4	5.786635672	5.795635754

(iii) Higher values of radiation parameter, Dufour number, and volumetric fractions have augmented fluid's thermal profiles.

(iv) Concentration of fluid has retarded with upsurge in Soret number and chemical reaction parameter, whereas growth in activation factor of energy has supported the growth in concentration.

(v) Motility of microorganisms has retarded by upsurge in the values of bioconvection Lewis and Peclet numbers.

(vi) It has been noticed that when K_r, M and Re varies from 0.2 to 0.6 then in case of nanofluid, skin friction changes from 0.288 to 0.633 at $\phi_1 = 0.01$ and from 0.292 to 0.646 at $\phi_1 = 0.02$ and in case of hybrid nanofluid the variations in skin friction are from 0.328 to 0.646 at $\phi_1,\phi_2 = 0.01$ and from 0.335 to 0.703 at $\phi_1,\phi_2 = 0.02$

(vii) Numerical influence of different factor upon various physical quantities of interest has been evaluated for single and double nanoparticles. It has revealed that thermal flow rate has augmented more in case of hybrid nanofluid.

Nomenclature

u, v, w: Dimensional velocity components (m/s)
p: Dimensional pressure (Pa)
δ: Microorganism concentration number
h: Channel height (m)
K_r: Rotation parameter
T: Dimensional temperature (K)
C_p: Specific heat ($J\,kg^{-1}K^{-1}$)
Nu: Nusselt number
C_f: Skin friction coefficient
Sh: Sherwood number
η: Similarity variable
k_T: Thermal diffusion ratio
Re: Reynolds number
Du: Dufour number
Pr: Prandtl number
τ: Temperature parameter
Rd: Radiation parameter
Sr: Soret number
E: Activation energy parameter
Sc: Schmidt number
Γ: Chemical reaction parameter
Lb: Bioconvection Lewis number
Pe: Peclet number
C: Dimensional concentration (kg/m^3).

Data Availability

The data that support the findings of this study are available from the corresponding author upon reasonable request.

Conflicts of Interest

The authors declare that they have no conflicts of interest.

Acknowledgments

The authors extend their appreciation to the Deanship of Scientific Research at King Khalid University, Abha, Saudi Arabia, for funding this work through the Research Group Project under grant number (RGP.2/300/44).

References

[1] A. J. Chamkha and A. Ben-Nakhi, "MHD mixed convection–radiation interaction along a permeable surface immersed in a porous medium in the presence of Soret and Dufour's effects," *Heat and Mass Transfer*, vol. 44, pp. 845–856, 2008.

[2] G. Rasool, A. Shafiq, and D. Baleanu, "Consequences of Soret–Dufour effects, thermal radiation, and binary chemical reaction on Darcy–Forchheimer flow of nanofluids," *Symmetry*, vol. 12, no. 9, Article ID 1421, 2020.

[3] S. A. Khan, T. Hayat, M. Ijaz Khan, and A. Alsaedi, "Salient features of Dufour and Soret effect in radiative MHD flow of viscous fluid by a rotating cone with entropy generation," *International Journal of Hydrogen Energy*, vol. 45, no. 28, pp. 14552–14564, 2020.

[4] K. Vafai, A. A. Khan, G. Fatima, S. M. Sait, and R. Ellahi, "Dufour, Soret and radiation effects with magnetic dipole on Powell-Eyring fluid flow over a stretching sheet," *International Journal of Numerical Methods for Heat & Fluid Flow*, vol. 31, no. 4, pp. 1085–1103, 2020.

[5] S. A. Khan, T. Hayat, and A. Alsaedi, "Irreversibility analysis in Darcy–Forchheimer flow of viscous fluid with Dufour and Soret effects via finite difference method," *Case Studies in Thermal Engineering*, vol. 26, Article ID 101065, 2021.

[6] M. B. Hafeez, W. Sumelka, U. Nazir, H. Ahmad, and S. Askar, "Mechanism of solute and thermal characteristics in a Casson hybrid nanofluid based with ethylene glycol influenced by Soret and Dufour effects," *Energies*, vol. 14, no. 20, Article ID 6818, 2021.

[7] G. C. Layek, B. Mandal, and K. Bhattacharyya, "Dufour and Soret effects on unsteady heat and mass transfer for Powell-Eyring fluid flow over an expanding permeable sheet," *Journal of Applied and Computational Mechanics*, vol. 6, no. 4, pp. 985–998, 2020.

[8] A. S. Kotnurkar and D. C. Katagi, "Thermo-diffusion and diffusion-thermo effects on MHD third-grade nanofluid flow driven by peristaltic transport," *Arabian Journal for Science and Engineering*, vol. 45, pp. 4995–5008, 2020.

[9] S. U. S. Choi and J. A. Eastman, "Enhancing thermal conductivity of fluids with nanoparticles," in *1995*

International Mechanical Engineering Congress and Exhibition, Argonne National Lab., IL (United States), 1995.

[10] M. Sheikholeslami, M. Hatami, and D. D. Ganji, "Nanofluid flow and heat transfer in a rotating system in the presence of a magnetic field," *Journal of Molecular Liquids*, vol. 190, pp. 112–120, 2014.

[11] Z. Said, P. Sharma, N. Aslfattahi, and M. Ghodbane, "Experimental analysis of novel ionic liquid-MXene hybrid nanofluid's energy storage properties: model-prediction using modern ensemble machine learning methods," *Journal of Energy Storage*, vol. 52, Part B, Article ID 104858, 2022.

[12] P. Sharma, Z. Said, A. Kumar et al., "Recent advances in machine learning research for nanofluid-based heat transfer in renewable energy system," *Energy & Fuels*, vol. 36, no. 13, pp. 6626–6658, 2022.

[13] L. Ahmad and M. Khan, "Numerical simulation for MHD flow of Sisko nanofluid over a moving curved surface: a revised model," *Microsystem Technologies*, vol. 25, pp. 2411–2428, 2019.

[14] S. Islam, A. Khan, W. Deebani, E. Bonyah, N. A. Alreshidi, and Z. Shah, "Influences of Hall current and radiation on MHD micropolar non-Newtonian hybrid nanofluid flow between two surfaces," *AIP Advances*, vol. 10, no. 5, Article ID 055015, 2020.

[15] Z. Said, P. Sharma, R. M. Elavarasan, A. K. Tiwari, and M. K. Rathod, "Exploring the specific heat capacity of water-based hybrid nanofluids for solar energy applications: a comparative evaluation of modern ensemble machine learning techniques," *Journal of Energy Storage*, vol. 54, Article ID 105230, 2022.

[16] Y.-X. Li, M. I. Khan, R. J. Punith Gowda et al., "Dynamics of aluminum oxide and copper hybrid nanofluid in nonlinear mixed Marangoni convective flow with entropy generation: applications to renewable energy," *Chinese Journal of Physics*, vol. 73, pp. 275–287, 2021.

[17] Z. Said, P. Sharma, A. K. Tiwari et al., "Application of novel framework based on ensemble boosted regression trees and Gaussian process regression in modelling thermal performance of small-scale Organic Rankine Cycle (ORC) using hybrid nanofluid," *Journal of Cleaner Production*, vol. 360, Article ID 132194, 2022.

[18] G. I. Taylor, "Experiments with rotating fluids," *Proceedings of the Royal Society of London. Series A, Containing Papers of a Mathematical and Physical Character*, vol. 100, no. 703, pp. 114–121, 1921.

[19] H. P. Greenspan, *The Theory of Rotating Fluids*, CUP Archive, 1968.

[20] M. Turkyilmazoglu, "Fluid flow and heat transfer over a rotating and vertically moving disk," *Physics of Fluids*, vol. 30, no. 6, Article ID 063605, 2018.

[21] L. K. Forbes, "Steady flow of a Reiner–Rivlin fluid between rotating plates," *Physics of Fluids*, vol. 30, no. 10, Article ID 103104, 2018.

[22] A. S. Dogonchi, D. D. Ganji, and O. D. Makinde, "Impact of stretching and penetration of walls on nanofluid flow and heat transfer in a rotating system," *Defect and Diffusion Forum*, vol. 387, pp. 37–50, 2018.

[23] S. Muhammad, S. I. A. Shah, G. Ali, M. Ishaq, S. A. Hussain, and H. Ullah, "Squeezing nanofluid flow between two parallel plates under the influence of MHD and thermal radiation," *Asian Research Journal of Mathematics*, vol. 10, no. 1, pp. 1–20, 2018.

[24] T. Salahuddin, M. Arshad, N. Siddique, and I. Tlili, "Change in internal energy of viscoelastic fluid flow between two rotating parallel plates having variable fluid properties," *Indian Journal of Physics*, vol. 95, pp. 1801–1811, 2021.

[25] A. R. Bestman, "Natural convection boundary layer with suction and mass transfer in a porous medium," *International Journal of Energy Research*, vol. 14, no. 4, pp. 389–396, 1990.

[26] N. S. Khan, P. Kumam, and P. Thounthong, "Second law analysis with effects of Arrhenius activation energy and binary chemical reaction on nanofluid flow," *Scientific Reports*, vol. 10, Article ID 1226, 2020.

[27] M. M. Bhatti and E. E. Michaelides, "Study of Arrhenius activation energy on the thermo-bioconvection nanofluid flow over a Riga plate," *Journal of Thermal Analysis and Calorimetry*, vol. 143, pp. 2029–2038, 2021.

[28] A. Khan, A. Saeed, A. Tassaddiq et al., "Bio-convective micropolar nanofluid flow over thin moving needle subject to Arrhenius activation energy, viscous dissipation and binary chemical reaction," *Case Studies in Thermal Engineering*, vol. 25, Article ID 100989, 2021.

[29] T. Muhammad, H. Waqas, S. A. Khan, R. Ellahi, and S. M. Sait, "Significance of nonlinear thermal radiation in 3D Eyring-Powell nanofluid flow with Arrhenius activation energy," *Journal of Thermal Analysis and Calorimetry*, vol. 143, pp. 929–944, 2021.

[30] M. Asma, W. A. M. Othman, and T. Muhammad, "Numerical study for Darcy–Forchheimer flow of nanofluid due to a rotating disk with binary chemical reaction and Arrhenius activation energy," *Mathematics*, vol. 7, no. 10, Article ID 921, 2019.

[31] R. Kumar, A. Bhattacharyya, G. S. Seth, and A. J. Chamkha, "Transportation of magnetite nanofluid flow and heat transfer over a rotating porous disk with Arrhenius activation energy: fourth order Noumerov's method," *Chinese Journal of Physics*, vol. 69, pp. 172–185, 2021.

[32] B. Ali, P. K. Pattnaik, R. A. Naqvi, H. Waqas, and S. Hussain, "Brownian motion and thermophoresis effects on bioconvection of rotating Maxwell nanofluid over a Riga plate with Arrhenius activation energy and Cattaneo–Christov heat flux theory," *Thermal Science and Engineering Progress*, vol. 23, Article ID 100863, 2021.

[33] D. U. Sarwe, B. Shanker, R. Mishra, R. S. Varun Kumar, and M. R. Raja Shekar, "Simultaneous impact of magnetic and Arrhenius activation energy on the flow of Casson hybrid nanofluid over a vertically moving plate," *International Journal of Thermofluid Science and Technology*, vol. 8, no. 2, Article ID 080202, 2021.

[34] S. A. Shehzad, T. Hayat, M. S. Alhuthali, and S. Asghar, "MHD three-dimensional flow of Jeffrey fluid with Newtonian heating," *Journal of Central South University*, vol. 21, pp. 1428–1433, 2014.

[35] L. Ahmad, S. Javed, M. I. Khan, M. Riaz Khan, E. R. El-Zahar, and A. A. A. Mousa, "Non-axisymmetric Homann stagnation-point flow of unsteady Walter's B nanofluid over a vertical cylindrical disk," *Proceedings of the Institution of Mechanical Engineers, Part E: Journal of Process Mechanical Engineering*, 2022.

[36] M. Usman, T. Gul, A. Khan, A. Alsubie, and M. Z. Ullah, "Electromagnetic couple stress film flow of hybrid nanofluid over an unsteady rotating disc," *International Communications in Heat and Mass Transfer*, vol. 127, Article ID 105562, 2021.

[37] L. Ahmad and M. Khan, "Importance of activation energy in development of chemical covalent bonding in flow of Sisko magneto-nanofluids over a porous moving curved surface,"

International Journal of Hydrogen Energy, vol. 44, no. 21, pp. 10197–10206, 2019.

[38] L. Ahmad, A. Munir, and M. Khan, "Locally non-similar and thermally radiative Sisko fluid flow with magnetic and Joule heating effects," *Journal of Magnetism and Magnetic Materials*, vol. 487, Article ID 165284, 2019.

[39] W. N. Mutuku and O. D. Makinde, "Hydromagnetic bioconvection of nanofluid over a permeable vertical plate due to gyrotactic microorganisms," *Computers & Fluids*, vol. 95, pp. 88–97, 2014.

[40] Z. Shah, S. Islam, T. Gul, E. Bonyah, and M. A. Khan, "The electrical MHD and Hall current impact on micropolar nanofluid flow between rotating parallel plates," *Results in Physics*, vol. 9, pp. 1201–1214, 2018.

[41] H. A. Attia and N. A. Kotb, "MHD flow between two parallel plates with heat transfer," *Acta Mechanica*, vol. 117, pp. 215–220, 1996.

[42] M. Sheikholeslami and D. D. Ganji, "Three dimensional heat and mass transfer in a rotating system using nanofluid," *Powder Technology*, vol. 253, pp. 789–796, 2014.

[43] M. Hatami, J. Hatami, and D. D. Ganji, "Computer simulation of MHD blood conveying gold nanoparticles as a third grade non-Newtonian nanofluid in a hollow porous vessel," *Computer Methods and Programs in Biomedicine*, vol. 113, no. 2, pp. 632–641, 2014.

[44] C. Zhang, L. Zheng, X. Zhang, and G. Chen, "MHD flow and radiation heat transfer of nanofluids in porous media with variable surface heat flux and chemical reaction," *Applied Mathematical Modelling*, vol. 39, no. 1, pp. 165–181, 2015.

[45] S.-J. Liao, "An explicit, totally analytic approximate solution for Blasius' viscous flow problems," *International Journal of Non-Linear Mechanics*, vol. 34, no. 4, pp. 759–778, 1999.

[46] S. Liao, "An optimal homotopy-analysis approach for strongly nonlinear differential equations," *Communications in Nonlinear Science and Numerical Simulation*, vol. 15, no. 8, pp. 2003–2016, 2010.